Swimming ability and flagellar motility of sperm packets of the volvocine green alga *Pleodorina starrii*

Short Title: Flagellar motility of sperm packets of *Pleodorina starrii*

Azusa Kage [1]*, Kohei Takahashi [2], Hisayoshi Nozaki [2], Tetsuya Higashiyama [2], Shoji A. Baba [3], Takayuki Nishizaka [1]

[1] Department of Physics, Gakushuin University, 1-5-1 Mejiro, Toshima-ku, Tokyo 171-8588, Japan

[2] Department of Biological Sciences, Graduate School of Science, The University of Tokyo, 7-3-1 Hongo, Bunkyo-ku, Tokyo 113-0033, Japan

[3] Department of Biology, Ochanomizu University, 2-1-1 Otsuka, Bunkyo-ku, Tokyo 112-8610, Japan

*Corresponding author. azusa.kage@gakushuin.ac.jp

Keywords

Eukaryotic flagella, Volvocales, low Reynolds number, microswimmer, collective motion

Abstract

Eukaryotic flagella collectively form metachronal waves and exhibit the ability to swim or cause flow. Large volvocine genera such as *Eudorina*, *Pleodorina*, and *Volvox* form bundles of small male gametes (sperm) called “sperm packets” for sexual reproduction. Although sperm packets have been reported to have flagella and the ability to swim, there has been no quantitative analysis of the motility of sperm packets. Moreover, describing motility of sperm packets is important in the context of collective motion and low Reynolds-number biofluid dynamics. In this study, we quantitatively described the swimming behavior of the sperm packets of a male strain of *Pleodorina starrii*. Although smaller, sperm packets swam faster than the asexual colonies of the same male strain. Sperm packets swam approximately 1.4 times faster than asexual colonies. Body length was approximately 2.3 times larger in the asexual colonies than in the sperm packets. Analysis of flagellar waveforms revealed that flagella from sperm packets and asexual colonies showed ciliary-type motion, whereas flagella from dissociated single sperm showed flagellar-type motion, suggesting the presence of a switching mechanism between sperm packets and dissociated sperm. Flagella from sperm packets were approximately 0.5 times shorter and had a beat period approximately twice as long as those from asexual colonies. The flagella of sperm packets were densely distributed over the anterior part of the body, whereas the flagella of asexual colonies were sparse and evenly distributed. The effect of the distribution of flagella, but not the number of flagella, seemed to illustrate the significant difference in the speeds between sperm packets and asexual colonies.

Introduction

Collective motion is common in nature, such as in schools of fish [1], flocks of birds [2] or herds of sheep [3]. In the case of low Reynolds number (Re<<1), metachronal waves of eukaryotic flagella or cilia [4,5] are a form of collective motion of many flagella/cilia and are important for microbial swimming and flow generation inside the animal body.

Volvocine green algae, ranging from unicellular *Chlamydomonas* [6], 4-celled *Tetrabaena* [7] to thousands-celled *Volvox* [8,9], have been used as model organisms to investigate the dynamics of multiple flagella. They have two equal-length flagella in one cell, and flagella in the entire body have been shown to move collectively in many cases. Previous studies on the motility of multicellular volvocines focused on asexual colonies that are in their usual form in culture. Although they have been known to sexually reproduce [10], the function of motility in sexual reproduction in multicellular volvocines remains unclear.

In the process of sexual reproduction, bundles of small male gametes or sperm called “sperm packets” have been reported in large multicellular volvocine genera such as *Eudorina* [11], *Pleodorina* [12,13] and *Volvox* [14,15]. Male gametes or sperm in these genera are characterized as biflagellated cells with elongated cell bodies. Sperm are bundled as packets in male colonies, and these sperm packets swim into female colonies [12,13]. Sperm packets subsequently dissociate into single sperm after arrival at the female colonies. These processes have only been described qualitatively, and no study has quantitatively characterized the movement of flagella in sperm packets or sperm.

In this study, we focused on the motility of sperm packets in the volvocine alga *Pleodorina starrii* (Figure 1). *P. starrii* has three sexes: male, female and hermaphrodite [16]. We focused on the male strain and compared the swimming and flagellar motions of sperm packets with those of asexual colonies. We found that the swimming speed of asexual colonies was approximately 0.7 times lower than that of sperm packets, whereas the body size in asexual colonies was approximately 2.3 times larger than that in sperm packets. A comparison with a previous computational study suggested that the distribution of flagella illustrates the difference in swimming

speeds between sperm packets and asexual colonies. Furthermore, we found that flagella from a single dissociated sperm showed flagellar-type motion, whereas flagella from sperm packets showed ciliary-type motion, suggesting a waveform switching mechanism in sperm cells. Our findings provide insights into the function of motility in the sexual reproduction of volvocines, which had previously been overlooked.

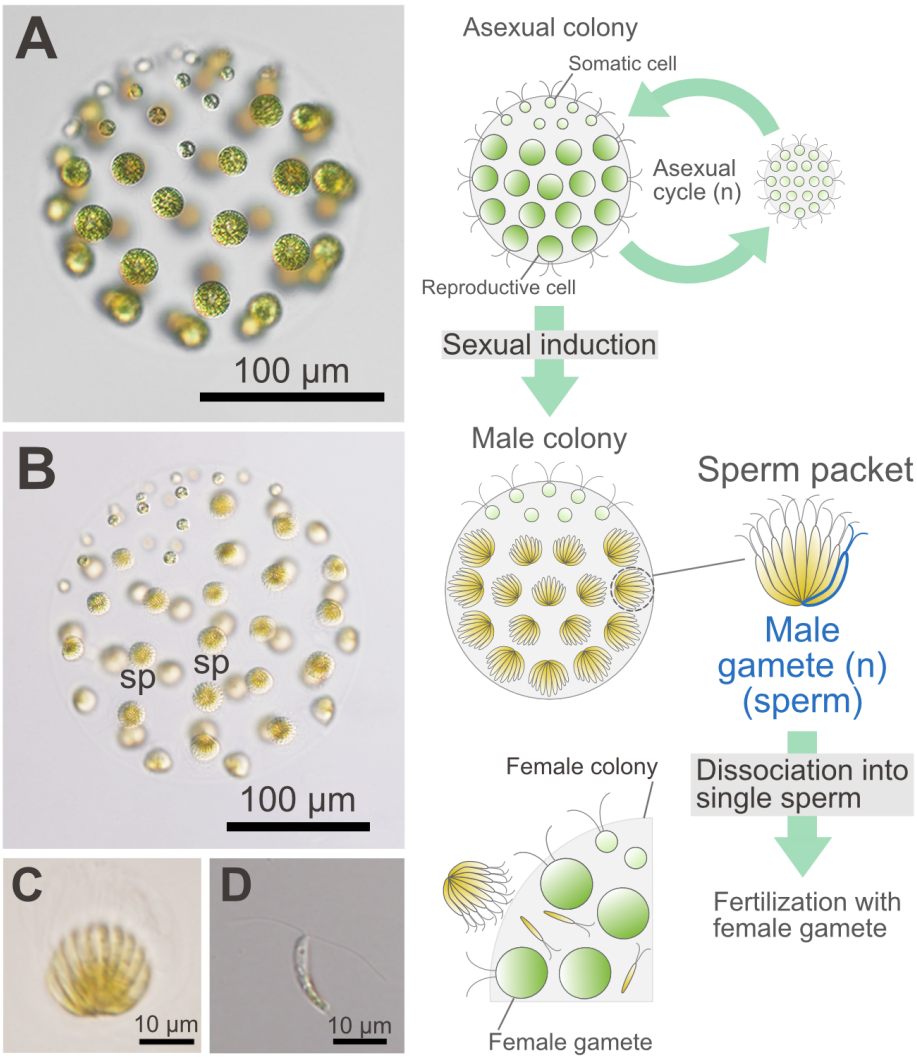

Fig. 1. Schematic representation of the life cycle of *Pleodorina starrii*. In general, the colonies proliferate asexually. Each colony consists of 32–64 cells with equal-length flagella. The cycle of sexual reproduction begins under a lack of nitrogen, and consequently, male colonies with sperm packets—bundles of male gametes (sperm) with two equal-length flagella—are formed. (A) 64-celled mature asexual colony. (B) Sexually induced male colony with sperm packets (sp). (C) Sperm packet. (D) Dissociated single sperm.

Materials and Methods

Culture

Pleodorina starrii was maintained at 20 °C in the AF6 medium under a 10:14 light/dark (LD) cycle. Asexual colonies were transferred into the Volvox thiamine acetate (VTAC) medium and incubated for 2-3 days at 25 °C under a 12:12 LD cycle. Sperm packets were induced by transferring 3-day colonies from the VTAC medium into the mating medium [12,16]. The unisex male strain P7 [16] (=NIES-4480 [17]) was used unless otherwise stated. The dissociation process of the sperm packet was observed using the unisex male strain P7×P10 F1-14, which is the offspring of P7. The experiments were performed at temperature of approximately 23-25 °C during the subjective daytime.

Recording of free swimming

Swimming activity was recorded using an upright microscope BX53 (Olympus, Tokyo, Japan) with a halogen lamp (Olympus, Tokyo, Japan), dry dark-field condenser (U-DCD, Olympus, Tokyo, Japan), and 620-nm long-pass filter (SCF-50S-62R, OptSigma, Tokyo, Japan). Although phototaxis was not examined in the present study, the wavelength was chosen based on the studies on *Chlamydomonas* phototaxis, which did not induce phototaxis in *Chlamydomonas* [18]. *P. starrii* was confined between a glass slide (S1126, Matsunami, Osaka, Japan) and a coverslip (18×18 mm, Matsunami, Osaka, Japan) with a ~10×10 mm square hole in a 0.5 mm silicone rubber spacer (Kogugo, Tokyo, Japan). Movies were captured at 14.3 fps using a CMOS camera (UI-3250-CP, IDS, Obersulm, Germany) to monitor swimming and at 1000 fps using a high-speed CMOS camera (VCC-H1540, Digimo, Tokyo, Japan) to monitor flagellar motility. A 10x objective lens (NA 0.40) was used to observe sperm packets, whereas a 4x objective lens (NA 0.13) was used to observe asexual colonies. Swimming trajectories and body lengths were quantified using the TrackMate plugin [19] in ImageJ (Fiji). The swimming speed of each individual was calculated as the mean swimming speed along the trajectory. The minimum value of the estimated diameter in the track was

107 considered as the body length because the estimated diameter was the minimum when the object
108 was in focus. Flagellar motility during swimming was visualized using the same setup (objective
109 10x) except that a mercury lamp (Olympus, Tokyo, Japan) without a long-pass filter (i.e., white light)
110 was used.
111
112 **Recording of flagellar motility of sperm packets**
113 To visualize flagellar movement, sperm packets were captured using a glass micropipette [20].
114 Glass pipettes with a tip diameter of ~20 μm were fabricated with the puller (PC-100, Narishige,
115 Tokyo, Japan) and the microforge (MF2, Narishige, Tokyo, Japan) from the capillary (G-1,
116 Narishige, Tokyo, Japan). The glass pipette was set to the injector (IM-11-2, Narishige, Tokyo,
117 Japan) on an inverted microscope (IX71, Olympus, Tokyo, Japan), 0.5–2 μL droplets of the culture
118 medium were placed on a glass-bottom dish (P50G-0-30-F, Mattek, Ashland, MA, US), and the
119 object inside the droplet was suctioned with the pipette. The droplets were covered with mineral oil
120 (8042-47-5; ICN Biomedicals, Aurora, OH, US) to prevent vaporization during observation. Movies
121 were captured at 1000 fps using a high-speed CMOS camera (VCC-H1540, Digimo, Tokyo, Japan),
122 long-working distance phase-contrast optics (Olympus, Tokyo, Japan) and a 40x objective lens (NA
123 0.75).
124
125 **Analysis of flagellar motility**
126 The flagellar waveform was analyzed using the lab-made software Bohboh [21]. Semi-auto-tracking
127 of flagella was applied to the dark-field images of asexual colonies and dissociated single sperm.
128 For pipette-captured sperm packets, phase-contrast images of the flagella were tracked manually
129 because of poor contrast. From the time series of flagellar traces, we obtained 3D plots of curvature,
130 along with flagellar length and time [22]. Flagellar beat periods were visually estimated from the 3D
131 plots, and flagellar lengths were calculated from traces on Bohboh. Because the length fluctuated
132 along the beat period owing to the three-dimensionality of the waveform, the mean length for each
133 flagellum (50–100 frames) was adopted its flagellar length.
134

135 **Immunofluorescence microscopy**

136 To visualize the distribution of flagella, indirect immunofluorescence microscopy was performed
137 according to Matsuura et al. [23], using the same method as that used for staining *Chlamydomonas*
138 flagella. The samples were fixed in methanol. Antiacetylated α-tubulin (mouse monoclonal 6-11B-1,
139 ab24610, Abcam, Cambridge, UK) diluted in blocking buffer to 1:500 was used as the primary
140 antibody, and samples were incubated with the primary antibody at 37 °C for 1 h. DyLight® 488-
141 conjugated goat anti-mouse IgG (ab96871, Abcam, Cambridge, UK) diluted in blocking buffer to
142 1:500 was used as the secondary antibody, and samples were incubated with the secondary
143 antibody at 37 °C for 1 h. Nuclei were stained with 50 μg/mL Hoechst 33342 (Nacalai Tesque,
144 Kyoto, Japan) in PBS before immunofluorescence staining. Confocal images were captured using
145 an FV-3000 microscope (Olympus, Tokyo, Japan) equipped with a 100x oil-immersion objective
146 lens (NA 1.50) at the Department of Life Sciences, Gakushuin University.

147

148 ## Results

149 **Sperm packets swam faster than asexual colonies**

150 To characterize the swimming of sperm packets, we recorded and compared the swimming of
151 sperm packets with asexual colonies of the same male strain (P7) at low magnification. Figure 2A
152 shows the relationship between swimming speed and body length of sperm packets (n = 185) and
153 asexual colonies (n = 313). Sperm packets had smaller body lengths and higher swimming speeds
154 than asexual colonies. The top and right panels of Figure 2A show the distribution of the diameters
155 and swimming speeds of sperm packets and asexual colonies. The diameters of sperm packets and
156 asexual colonies were 24.7 ± 5.9 μm (mean ± S.D., n = 185) and 54.7 ± 14.9 μm (mean ± S.D., n =
157 313), respectively. The swimming speeds of sperm packets and asexual colonies were 308 ± 73
158 μm/s (mean ± S.D., n = 185) and 215 ± 63 μm/s (mean ± S.D., n = 313), respectively, indicating that
159 sperm packets swam approximately 1.4 times faster than asexual colonies. Figures 2B and 2C
160 show the swimming trajectories of the sperm packets and asexual colonies, respectively. Both
161 exhibited nearly straight trajectories within an observation field of less than 1 mm.

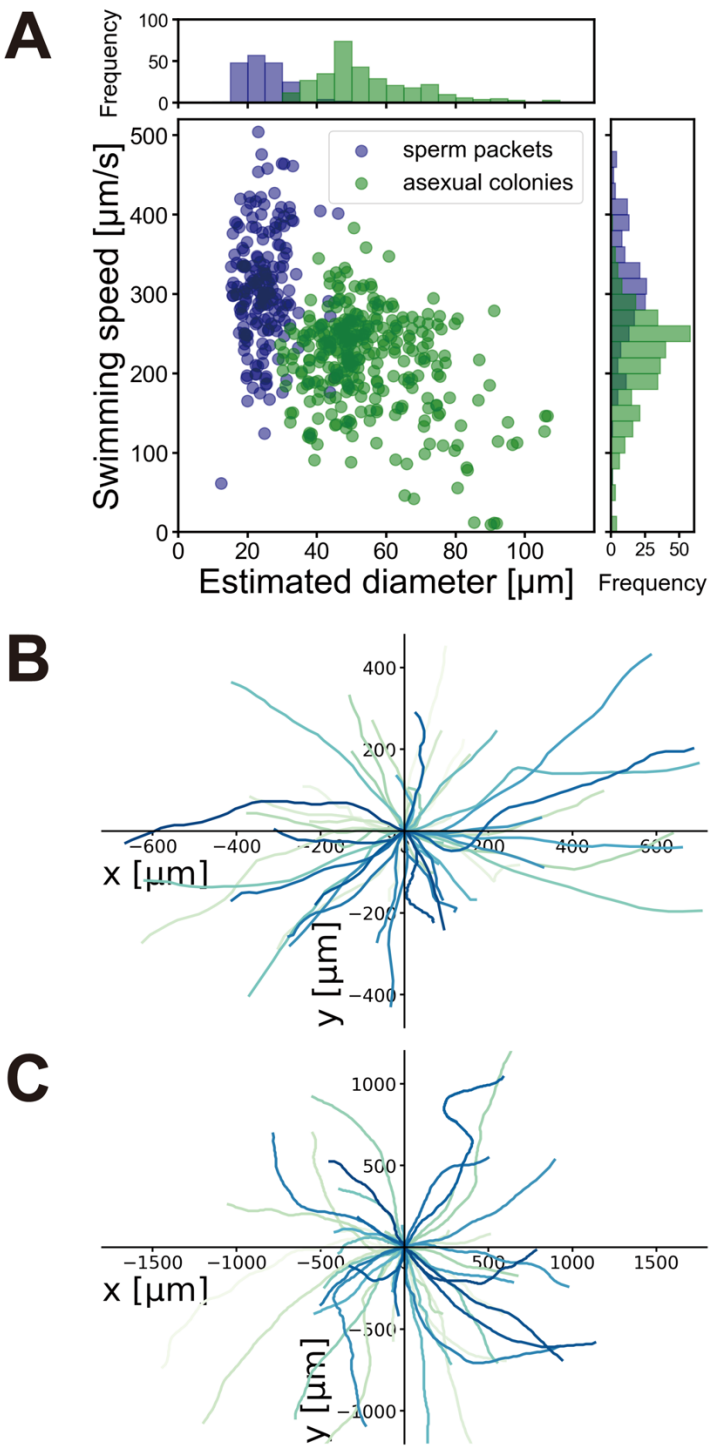

Fig. 2. Swimming of sperm packets and asexual colonies. (A) Swimming speed plotted against the body diameter. Top panel shows the histogram of diameter, and right panel shows the histogram of swimming speed (navy: sperm packets, green: asexual colonies). (B) Swimming trajectories of sperm packets. Twenty randomly chosen trajectories are shown. (C) Swimming trajectories of asexual colonies. Twenty randomly chosen trajectories are shown.

Visualization of flagella in dark-field microscopy

To clarify the reason for the difference in speed between sperm packets and asexual colonies, we visualized their flagellar movements. Figure 3 (as well as Supplementary Movie S1) shows a swimming sperm packet viewed from the side using a dark-field microscope. We observed that the sperm packet swam with flagella anterior and metachronal waves of the flagella traveling from the top region to the periphery of the packet, although it was difficult to determine the relationship between the direction of the wave and the power stroke of the flagella because of the dense distribution of flagella. The flagella of asexual colonies (Figure 4, Supplementary Movie S2) were evenly distributed over the body, and the metachronal waves were symplectic, i.e., the waves propagated in the same direction as the power stroke of the flagella [24], as observed in *Volvox* [25].

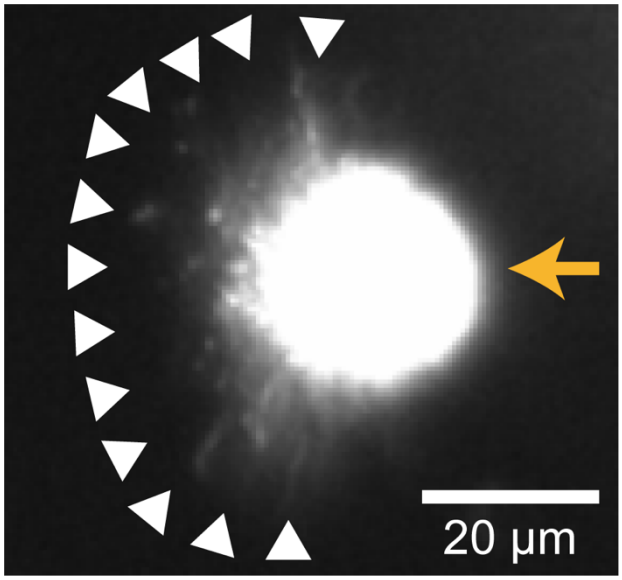

Fig. 3. Image of a sperm packet (side view) under dark-field microscopy. The sperm packet thrust itself with flagella anterior. The metachronal wave propagated from the center (see Supplementary Movie 1). White triangles indicate flagella, and the orange arrow indicates the swimming direction.

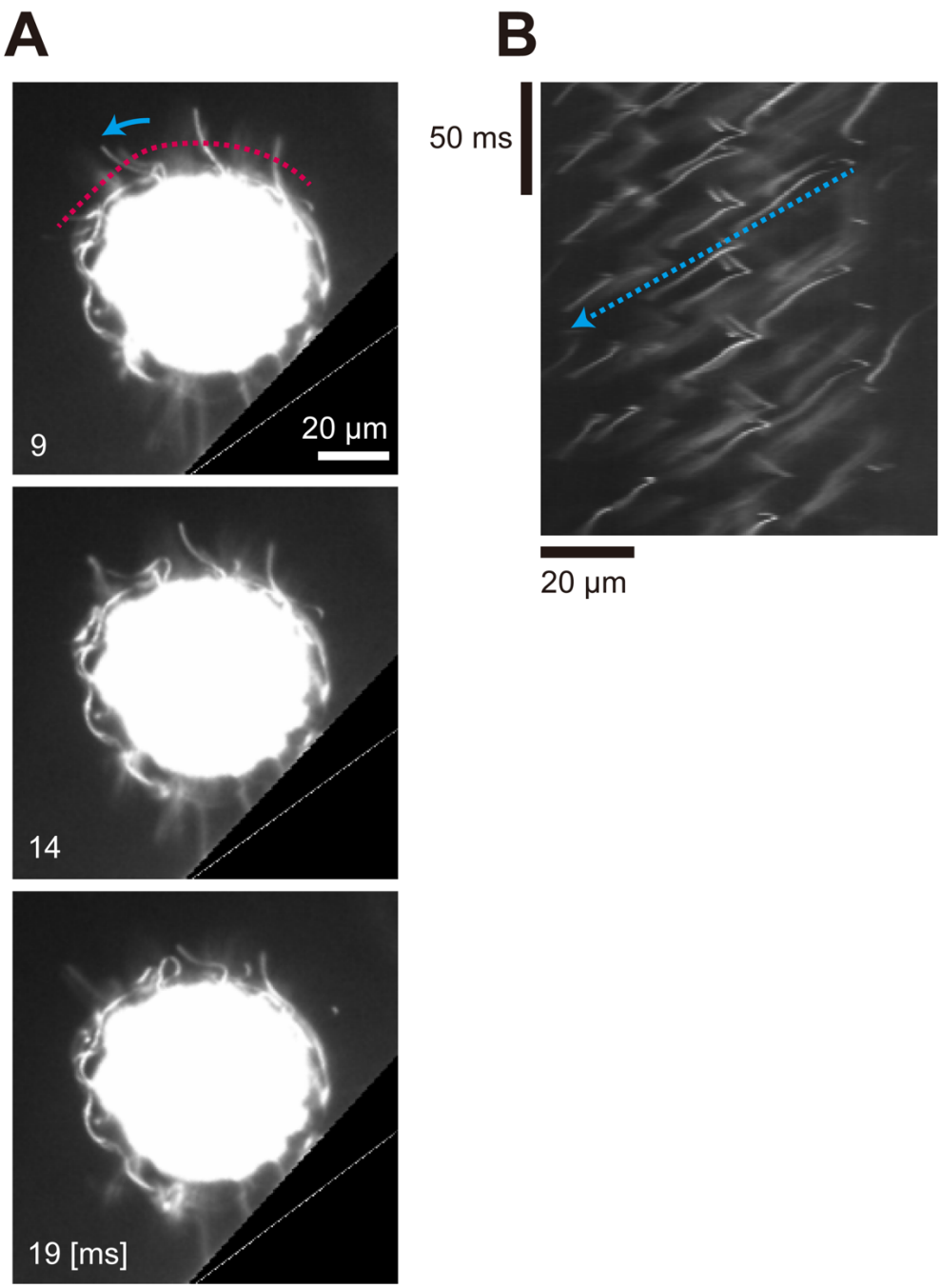

Fig. 4. An asexual colony in dark-field microscopy. (A) Images of an asexual colony. Flagella beat with ciliary-type motion. Registered images of a rolling colony near the wall are shown every 5 ms. The image of the silicone rubber spacer (wall) was deleted (black triangle in the lower right) for proper registration (see Supplementary Methods). Blue arrow indicates the direction of the effective stroke. Red broken line indicates where the kymograph (B) was drawn. Time [ms] corresponds to the time axis in (B). (B) Kymograph of the movement of flagella drawn from red broken line in (A). Blue broken arrow indicates the propagation of metachronal waves.

Sperm packets disassemble into a single sperm after arrival in the female colonies [13]. Figure 5 (Supplementary Movie S3) shows the process of disassembling a sperm packet, as recorded by dark-field microscopy. The packet disassembled gradually as the sperm moved randomly. To date, the trigger for this dissociation has not been identified. Figure 6 (Supplementary Movie S4) shows a single sperm after disassembly of a packet. The two flagella of the sperm beat alternately, and individual sperm barely propel themselves. Flagellar movement was flagellar-type, i.e., the flagella bent in two directions [26], similar to human or sea urchin sperm.

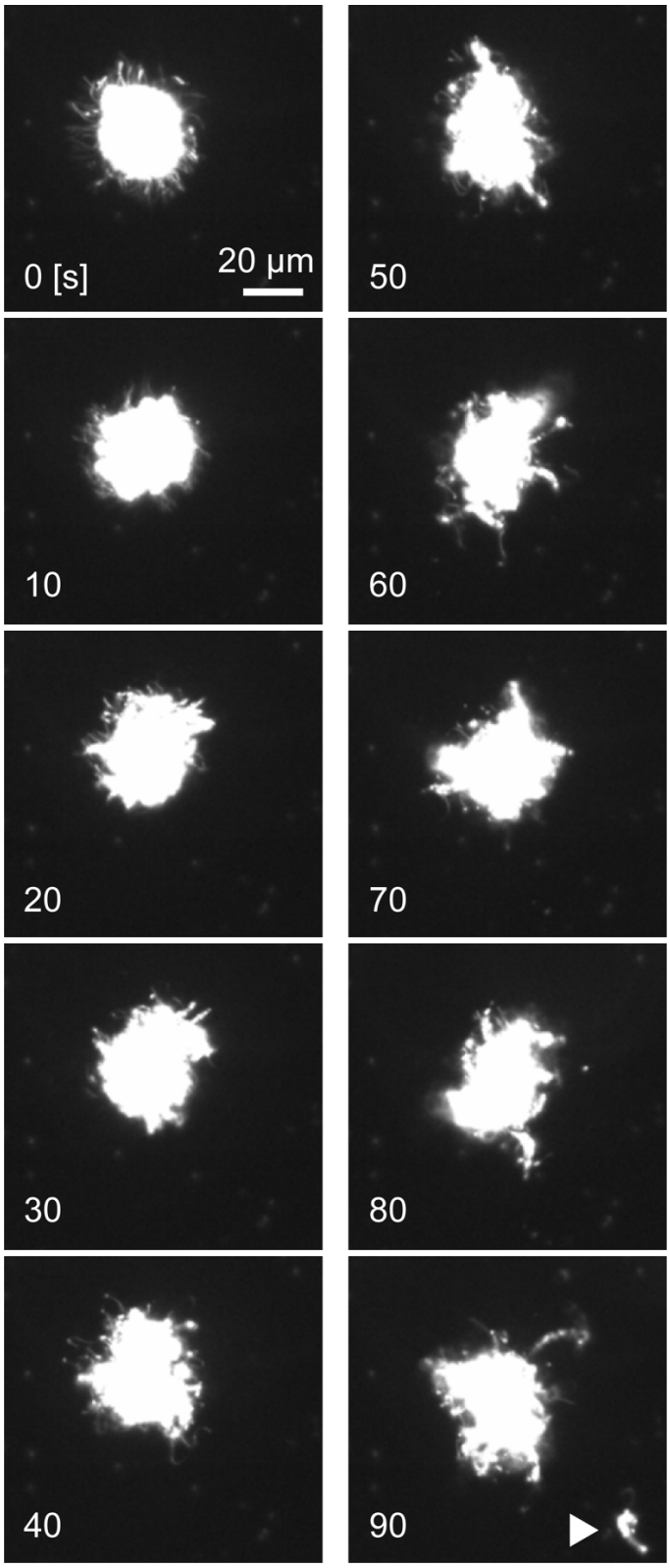

Fig. 5. Dissociation of a sperm packet viewed using dark-field microscopy. The sperm packet gradually collapsed, and the dissociated sperm jumped out of the packet. Images are shown every 10 s. White triangle indicate dissociated sperm.

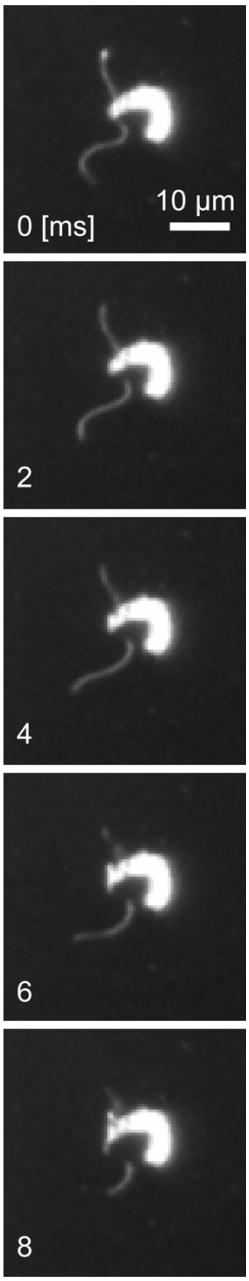

Fig. 6. Dark-field microscopy images of a single dissociated sperm. The two flagella beat with flagellar-type motion and did not synchronize. Images are shown every 2 ms.

Visualization of flagella of sperm packets held on the micropipette

Because it was difficult to analyze flagellar motility from freely moving sperm packets (Figure 3), we suctioned the sperm packets into a glass micropipette. Figure 7 (Supplementary Movie S5) shows the flagellar motility of a sperm packet held on a micropipette, using phase-contrast microscopy. We found that the flagella beat with a ciliary-type motion, i.e., the flagella bent in only one direction. The

effective stroke was directed from the top (anterior) region of the body to the periphery, and the metachronal waves were also directed from the top to the periphery. Thus, the metachronal waves in the sperm packets were symplectic, similar to those in asexual colonies.

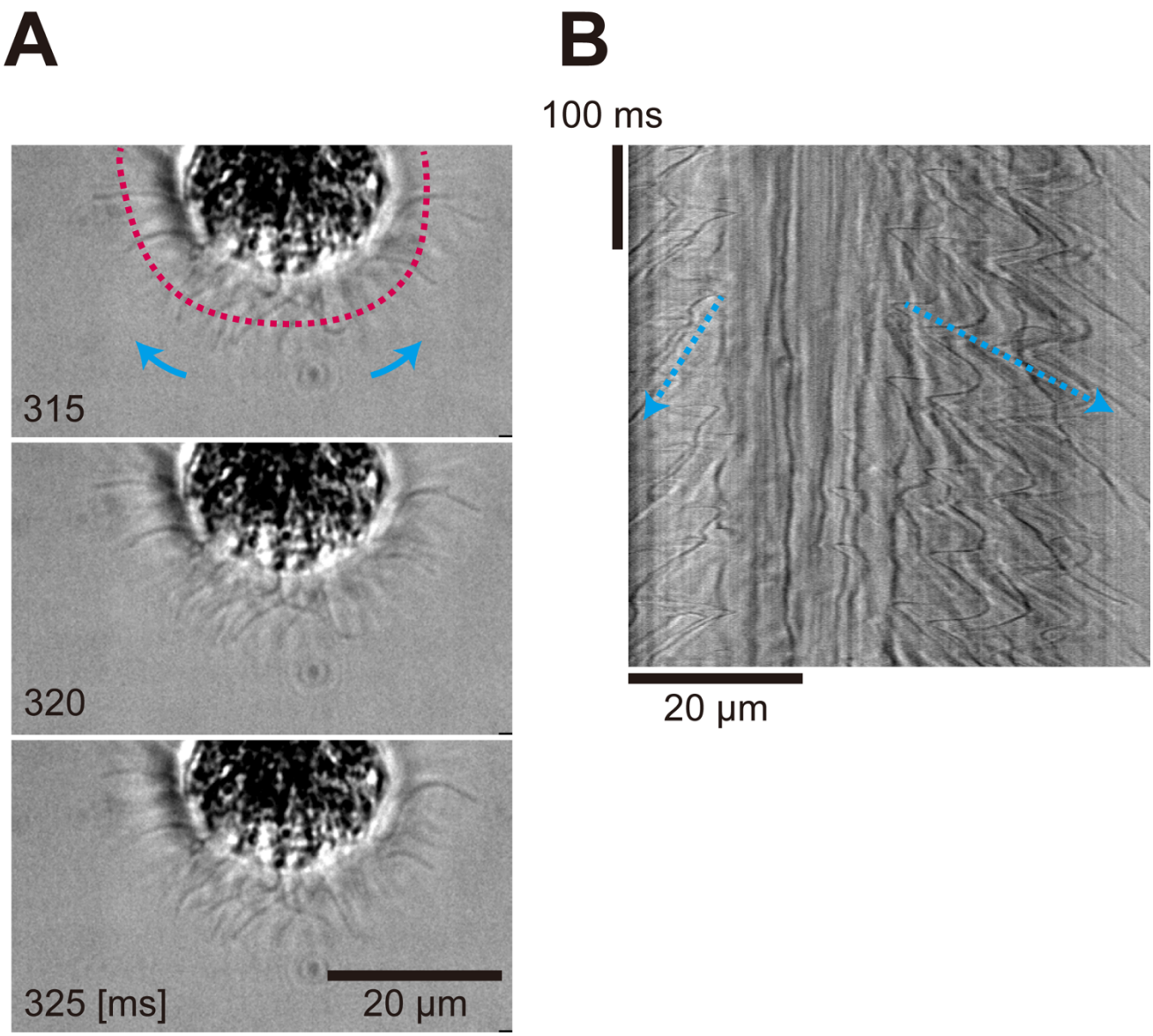

Fig. 7. A sperm packet captured to a micropipette in phase-contrast microscopy. (A) Images of a sperm packet. The flagella beat with ciliary-type motion. Images are shown every 5 ms. Blue arrows indicate the direction of effective stroke, and red broken line indicates where the kymograph (B) was drawn. Time [ms] corresponds to the time axis in (B). Contrast enhanced. (B) Kymograph of the movement of flagella drawn from the red broken line in (A). Blue broken arrows indicate the propagation of metachronal waves.

225 **Analysis of flagellar waveform**

226 We tracked and quantified flagellar movement. Figures 8A–C show a time series of flagellar
227 waveforms traced from an asexual colony (Figure 4), dissociated single sperm (Figure 6), and
228 sperm packets (Figure 7), respectively. The flagellum from the asexual colonies (Figure 8A) showed
229 ciliary-type movement, bending in one direction, similar to the colonies of other Volvocales [9]. The
230 flagellum from the dissociated single sperm (Figure 8B) showed flagellar-type movement with
231 principal and reverse bends [26]. The flagellum from sperm packets (Figure 8C) showed ciliary-type
232 motion with a usually larger period. The flagellum appeared shorter in sperm packets than in single
233 sperm or colonies. As shown in Figure 8D–F, 3D plots of curvature along with time and flagellar
234 length supported these views; Figures 8D and 8F indicate that the flagella from the asexual colony
235 and the sperm packet bent in only one direction (i.e., ciliary-type motion), whereas Figure 8E shows
236 that the flagella from the single dissociated sperm bent in two directions (i.e., flagellar-type motion).

237 Using waveform analysis (Figure 8, Supplementary Figure S1 and S2), we estimated the
238 beat period and length of the flagella (Supplementary Table 1). The beat period was 35 ± 13 ms in
239 asexual colonies (mean ± S.D., n = 4), 30 ± 9 ms in single dissociated sperm (n = 3) and 69 ± 18 ms
240 in sperm packets (n = 3). The flagellar length was 23.6 ± 8.1 μm in asexual colonies (n = 4), 16.4 ±
241 1.4 μm in single dissociated sperm (n = 3), and 11.0 ± 0.5 μm in sperm packets (n = 3).

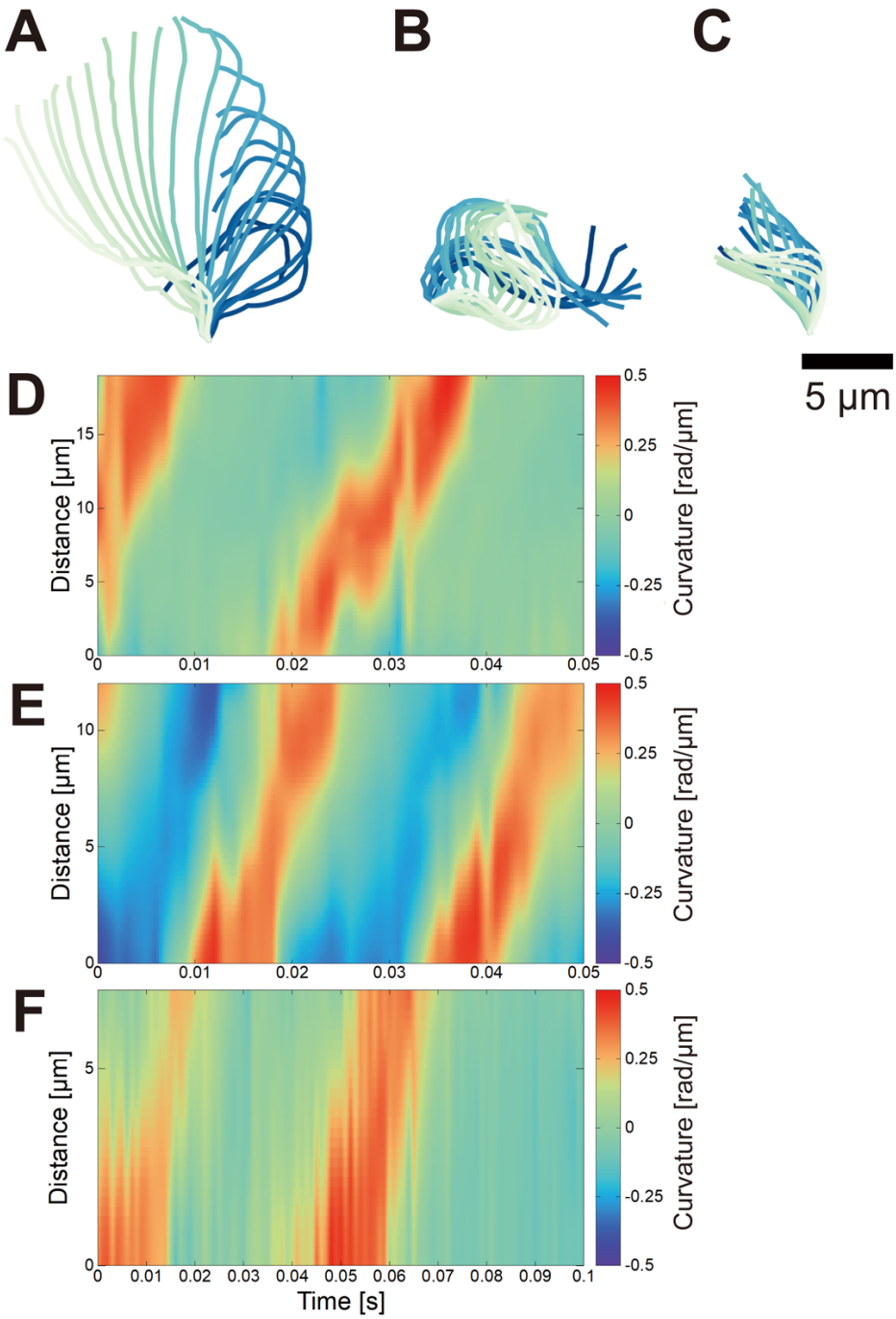

Fig. 8. Flagellar waveform of (A) an asexual colony, (B) a single dissociated sperm, and (C) a sperm packet. (A) and (B) show 20 frames in 1000 fps. (C) shows 60 frames every 3 frames. (D)–(F) 3D plots of curvature along with time and flagellar length obtained from (A)–(C). Ciliary-type waveform (D) and (F) show stripes of curvature of plus value (red) and near-zero (green), indicating a one-directional bend, whereas flagellar-type waveform (E) shows stripes of plus- (red) and minus-value (blue) curvature, indicating a two-directional bend.

250 **Visualization of the distribution of flagella**

251 Indirect immunofluorescence microscopy was used to clearly visualize the distribution of flagella.
252 Figures 9A and 9B show the distribution of flagella (green) in sperm packets and asexual colonies,
253 respectively. The flagella of sperm packets were densely distributed over the anterior part of the
254 body, whereas the flagella of asexual colonies were sparse and evenly distributed.

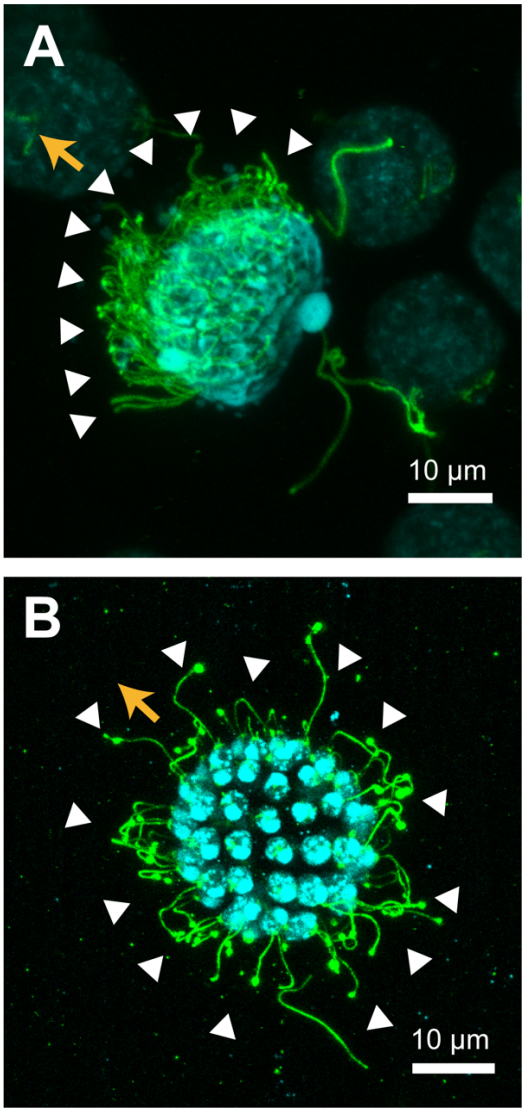

255

256 **Fig. 9.** Distribution of flagella in immunofluorescence microscopy. (A) A sperm packet; (B) an
257 asexual colony. Green structures represent acetylated α-tubulin (flagella), and blue structure
258 represents the nuclei. Z projections of confocal images are shown. White triangles indicate flagella,
259 and orange arrows indicate the swimming direction. Note that flagella were densely distributed in
260 the sperm packet, whereas the asexual colony had sparse distribution of flagella.

261

Discussion

The normalized body length is nearly the same, but the normalized speed is dramatically different between sperm packets and asexual colonies

Table 1 summarizes the swimming parameters of the sperm packets and asexual colonies. We found that, on average, asexual colonies had approximately 2.3 times larger diameter, approximately 0.7 times lower speed, 2.1 times larger flagellar length, and 0.5 times smaller beat period than sperm packets. Asexual colonies contained 32–64 cells [13], whereas the sperm packets contained 20–50 cells (n = 3). Thus, it is reasonable to assume that the number of flagella is comparable between the asexual colonies and sperm packets. From the numerical simulation of ciliated spherical bodies, Omori et al. [27] showed that the normalized swimming speed $\overline{U}/(\frac{L}{T})$, where $\overline{U}$ is the swimming speed, L is flagellar length, and T is flagellar beat period, decreased with the power of -2 of the normalized body length 2a/L (where a is the radius) if the number of the flagella N is fixed in 2a/L ranging 10 to 30. If we consider the mean flagellar length of each category, sperm packets and asexual colonies have a 2a/L of 2.2 and 2.3, respectively, which is nearly the same. However, the normalized swimming speed $\overline{U}/(\frac{L}{T})$ is dramatically different between the two categories, although both are approximately in quantitative agreement with the curves reported in [27] if we extrapolate. If the normalized body size and direction of the metachronal waves (symplectic or antiplectic) were the same, the number of flagella would cause a difference in swimming speed [27]. However, the number of flagella would not differ in our case. Thus, in our study, the difference in speed could be attributed to the difference in the distribution of flagella (Figure 9), which was not considered in [27]. Because the cell shape is elongated in sperm packets but spherical in asexual colonies [12,13,16], the spacing of the flagella would be smaller in sperm packets.

	Flagellar length, L [μm]	Flagellar period, T [ms]	L/T [μm/s]	Body length, 2a [μm]	Swimming speed, $\overline{U}$ [μm/s]	Normalized body length, 2a/L	Normalized speed, $\overline{U}/(\frac{L}{T})$
Sperm packets	11.0±0.5 (n=3)	69±18 (n=3)	167±44 (n=3)	24.7±5.9 (n=185)	308±73 (n=185)	2.2	1.8
Asexual colonies	23.6±8.1 (n=4)	35±13 (n=4)	649±69 (n=4)	54.7±14.9 (n=313)	215±63 (n=313)	2.3	0.3

Table 1. Swimming parameters of sperm packets and asexual colonies.

Although the beat period of sperm packets was longer than that of asexual colonies (i.e., the flagellar beat was slower in sperm packets), swimming was faster in sperm packets than in asexual colonies. This could be attributed to the size difference between sperm packets and asexual colonies as well as the difference in the waveform and collective motion of the flagella. The effect of size difference, i.e., sperm packets were smaller in size and thus had smaller drag than asexual colonies, might be stronger than the effect of the beat period difference. Another reason might be the differences in flagellar motion. Although flagellar movements of both sperm packets and asexual colonies were categorized as ciliary-type motion, they showed subtle differences in actual waveforms (Figure 8A and C) or spatiotemporal dynamics in curvatures (Figure 8D and F). These differences, as well as the differences in metachronal wave dynamics (Figure 4B, Figure 7B) and hydrodynamic interactions between flagella, would result in faster swimming in sperm packets.

Switching mechanism of flagellar- and ciliary-type motion

We found that the flagellar waveform changed in sperm packets and dissociated single sperm. Sperm packets showed ciliary-type movement, whereas dissociated single sperm showed flagellar-type motion. Wild-type *Chlamydomonas* flagella usually show ciliary-type motion, and sometimes the waveform becomes flagellar-type, depending on the Ca^{2+} concentration inside the flagella [28,29]. A similar mechanism can be considered for waveform switching in the sperm of *P. starrii*:

306 the Ca^{2+} concentration is constantly higher in the flagella of dissociated single sperm than in the
307 sperm packets. To test this hypothesis, an experiment using demembranated cell models of both
308 sperm packets and dissociated single sperm is desirable.
309 If the Ca^{2+} concentration is consistently higher in dissociated single sperm than in sperm
310 packets, the underlying cause may be the higher viscous load in single sperm than in sperm
311 packets. Ca^{2+} influx may occur through mechanosensitive channels (e.g., [30]).
312
313 **Significance of larger swimming speed in sperm packets**
314 The sperm packets swam faster than the asexual colonies. To date, we have not measured the
315 speed of sexual reproduction in female colonies. However, it would be reasonable to assume that
316 the speed of female sexual colonies would not be significantly higher than that of asexual colonies
317 because the morphology does not change significantly between sexual and asexual colonies of
318 females [16]. If we consider that the speed of female sexual colonies is not significantly different
319 from that of male asexual colonies, the faster swimming of sperm packets would enable them to
320 catch up with female colonies during sexual reproduction. However, it remains unclear whether they
321 are attracted to females.
322
323 **Conclusions**
324 In this study, we quantitatively characterized the swimming and flagellar motility of sperm packets of
325 the volvocine green alga *Pleodorina starrii*. Two important changes in the flagellar properties during
326 male gametogenesis and gamete fusion were confirmed. The first is the change in flagellar
327 distribution during sperm packet formation, which allows the packets to approach the female sexual
328 colony at a high speed. The second is the change from ciliary- to flagellar-type motility for effective
329 fusion with the female gametes. Further studies should clarify the phototaxis and chemotaxis of
330 sperm packets, the mechanism of switching flagellar waveforms, and the entire process of sexual
331 reproduction in the context of swimming.
332

Acknowledgements

This study was supported by JSPS KAKENHI #21K20661 (A.K.).

We thank Dr. Masafumi Hirono (Hosei University) for the immunofluorescence staining protocol, Ms. Tomoka Sakamoto (Narishige) for technical help with the suction experiments, and Dr. Toshihiro Omori (Tohoku University) for discussions.

Author contributions

A.K. conceived the study. K.T., H.N., and T.H. prepared the samples. T.N. constructed the microscopy system. S.A.B. provided the software and developed the image analysis methods. A.K. performed the experiments and analyzed the data. A.K. drafted the manuscript, and A.K., K.T., H.N., and T.N. contributed to the final manuscript.

References

1. Parrish JK, Viscido SV, Grünbaum D. Self-organized fish schools: an examination of emergent properties. Biol Bull. 2002;202: 296–305. doi: 10.2307/1543482.

2. Attanasi A, Cavagna A, Del Castello L, Giardina I, Jelic A, Melillo S, et al. Emergence of collective changes in travel direction of starling flocks from individual birds' fluctuations. J R Soc Interface. 2015;12: 20150319. doi: 10.1098/rsif.2015.0319.

3. Azaïs M, Blanco S, Bon R, Fournier R, Pillot MH, Gautrais J. Traveling pulse emerges from coupled intermittent walks: A case study in sheep. PLOS ONE. 2018;13: e0206817. doi: 10.1371/journal.pone.0206817.

4. Aiello E, Sleigh MA. The metachronal wave of lateral cilia of *Mytilus edulis*. J Cell Biol. 1972;54: 493–506. doi: 10.1083/jcb.54.3.493.

5. Narematsu N, Quek R, Chiam KH, Iwadate Y. Ciliary metachronal wave propagation on the compliant surface of *Paramecium* cells. Cytoskeleton (Hoboken). 2015;72: 633–646. doi: 10.1002/cm.21266.

359 6. Wan KY, Goldstein RE. Coordinated beating of algal flagella is mediated by basal coupling.
360 Proc Natl Acad Sci U S A. 2016;113: E2784-E2793. doi: 10.1073/pnas.1518527113.

361 7. Tanno A, Tokutsu R, Arakaki Y, Ueki N, Minagawa J, Yoshimura K, et al. The four-celled
362 Volvocales green alga *Tetrabaena socialis* exhibits weak photobehavior and high-
363 photoprotection ability. PLOS ONE. 2021;16: e0259138. doi: 10.1371/journal.pone.0259138.

364 8. Brumley DR, Wan KY, Polin M, Goldstein RE. Flagellar synchronization through direct
365 hydrodynamic interactions. eLife. 2014;3: e02750. doi: 10.7554/eLife.02750.

366 9. Ueki N, Wakabayashi KI. Detergent-extracted *Volvox* model exhibits an anterior-posterior
367 gradient in flagellar Ca2+ sensitivity. Proc Natl Acad Sci U S A. 2018;115: E1061–E1068. doi:
368 10.1073/pnas.1715489115.

369 10. Nozaki H. Morphology and evolution of sexual reproduction in the Volvocaceae (Chlorophyta).
370 J Plant Res. 1996;109: 353–361. doi: 10.1007/BF02344484.

371 11. Goldstein M. Speciation and mating behavior in *Eudorina*. J Protozool. 1964;11: 317–344. doi:
372 10.1111/j.1550-7408.1964.tb01762.x.

373 12. Nozaki H, Kuroiwa H, Mita T, Kuroiwa T. *Pleodorina japonica* sp. nov. (Volvocales,
374 Chlorophyta) with bacteria-like endosymbionts. Phycologia. 1989;28: 252–267. doi:
375 10.2216/i0031-8884-28-2-252.1.

376 13. Nozaki H, Ott FD, Coleman AW. Morphology, molecular phylogeny and taxonomy of two new
377 species of *Pleodorina* (volvoceae, Chlorophyceae) 1. J Phycol. 2006;42: 1072–1080. doi:
378 10.1111/j.1529-8817.2006.00255.x.

379 14. Darden WH Jr. Sexual differentiation in *Volvox aureus*. J Protozool. 1966;13: 239–255. doi:
380 10.1111/j.1550-7408.1966.tb01901.x.

381 15. Kochert G. Differentiation of reproductive cells in *Volvox carteri*. J Protozool. 1968;15: 438–452.
382 doi: 10.1111/j.1550-7408.1968.tb02154.x.

383 16. Takahashi K, Kawai-Toyooka H, Ootsuki R, Hamaji T, Tsuchikane Y, Sekimoto H, et al. Three
384 sex phenotypes in a haploid algal species give insights into the evolutionary transition to a self-
385 compatible mating system. Evolution. 2021;75: 2984–2993. doi: 10.1111/evo.14306.

386 17. Kawachi M, Ishimoto M, Mori F, Yumoto K, Sato M, M-HN. MCC-NIES. List of strains. 9th ed.
387 DVD. Tsukuba: National Institute for Environmental Studies; 2013.

388 18. Nultsch W, Throm G, Rimscha I. Phototactic investigations in *Chlamydomonas reinhardii*
389 dangeard in homocontinuous culture. Arch Microbiol. 1971;80: 351–369.

390 19. Tinevez JY, Perry N, Schindelin J, Hoopes GM, Reynolds GD, Laplantine E, et al. TrackMate:
391 an open and extensible platform for single-particle tracking. Methods. 2017;115: 80–90. doi:
392 10.1016/j.ymeth.2016.09.016.

393 20. de Maleprade H, Moisy F, Ishikawa T, Goldstein RE. Motility and phototaxis of *Gonium*, the
394 simplest differentiated colonial alga. Phys Rev E. 2020;101: 022416. doi:
395 10.1103/PhysRevE.101.022416.

396 21. Shiba K, Mogami Y, Baba SA. Ciliary movement of sea-urchin Embryos. Nat Sci Rep
397 Ochanomizu Univ. 2002;53: 49–54.

398 22. Iida T, Iwata Y, Mohri T, Baba SA, Hirohashi N. A coordinated sequence of distinct flagellar
399 waveforms enables a sharp flagellar turn mediated by squid sperm pH-taxis. Sci Rep. 2017;7:
400 12938. doi: 10.1038/s41598-017-13406-z.

401 23. Matsuura K, Lefebvre PA, Kamiya R, Hirono M. Bld10p, a novel protein essential for basal body
402 assembly in *Chlamydomonas*: localization to the cartwheel, the first ninefold symmetrical
403 structure appearing during assembly. J Cell Biol. 2004;165: 663–671. doi:
404 10.1083/jcb.200402022.

405 24. Knight-Jones EW. Relations between metachronism and the direction of ciliary beat in
406 Metazoa. J Cell Sci. 1954;s3–95: 503–521. doi: 10.1242/jcs.s3-95.32.503.

407 25. Brumley DR, Polin M, Pedley TJ, Goldstein RE. Metachronal waves in the flagellar beating of
408 *Volvox* and their hydrodynamic origin. J R Soc Interface. 2015;12: 20141358. doi:
409 10.1098/rsif.2014.1358.

410 26. Gibbons BH, Gibbons IR. Properties of flagellar “rigor waves” formed by abrupt removal of
411 adenosine triphosphate from actively swimming sea urchin sperm. J Cell Biol. 1974;63: 970–
412 985. doi: 10.1083/jcb.63.3.970.

413 27. Omori T, Ito H, Ishikawa T. Swimming microorganisms acquire optimal efficiency with multiple
414 cilia. Proc Natl Acad Sci U S A. 2020;117: 30201–30207. doi: 10.1073/pnas.2011146117.

415 28. Schmidt JA, Eckert R. Calcium couples flagellar reversal to photostimulation in
416 *Chlamydomonas reinhardtii*. Nature. 1976;262: 713–715. doi: 10.1038/262713a0.

417 29. Hyams JS, Borisy GG. Isolated flagellar apparatus of *Chlamydomonas*: characterization of
418 forward swimming and alteration of waveform and reversal of motion by calcium ions in vitro. J
419 Cell Sci. 1978;33: 235–253. doi: 10.1242/jcs.33.1.235.

420 30. Fujiu K, Nakayama Y, Iida H, Sokabe M, Yoshimura K. Mechanoreception in motile flagella of
421 *Chlamydomonas*. Nat Cell Biol. 2011;13: 630–632. doi: 10.1038/ncb2214.